

# Electronic Structure of $\text{Sr}_2\text{Cu}_2\text{ZnO}_2\text{S}_2$ Layered Oxysulfide with $\text{CuS}$ Layers

H. Hirose, K. Ueda,\* H. Kawazoe,<sup>†</sup> and H. Hosono

Materials and Structures Laboratory, Tokyo Institute of Technology, 4259, Nagatsuta, Midori, Yokohama, 226-8503, Japan

Received June 14, 2001. Revised Manuscript Received November 9, 2001

The electronic structure of p-type semiconducting  $\text{Sr}_2\text{Cu}_2\text{ZnO}_2\text{S}_2$  (SCZOS) was examined experimentally and theoretically. The band gap of SCZOS estimated by the optical absorption of its thin film was 2.7 eV, which is relatively large in chalcogenide semiconductors. Normal and inverse photoemission spectra were measured to observe the valence band or conduction band structure of this material. The observed band structure revealed that the Fermi level of SCZOS was located at the top of the valence band, and the bottom of the conduction band was approximately 2.5 eV above the Fermi level. These results demonstrate the wide-gap and p-type semiconducting nature of SCZOS. Comparison of the photoemission spectra with the density of states calculated by the tight-binding method led to the conclusion that the top of the valence band is mainly composed of a hybridized (Cu 3d)–(S 3p) band, and the bottom of the conduction band primarily consists of a dispersed Zn 4s band.

## Introduction

Layered compounds often show interesting physical properties such as superconductivity, colossal magnetoresistance, and charge density waves because of the two-dimensional structure of functional sublattices.<sup>1–3</sup> Recently, Zhu et al.<sup>4</sup> reported the preparation of a layered mixed-anion compound,  $\text{Sr}_2\text{Cu}_2\text{ZnO}_2\text{S}_2$  (SCZOS) oxysulfide, in which both oxygen and sulfur are divalent anions without forming oxoacid species such as  $\text{SO}_4^{2-}$  and  $\text{SO}_3^{2-}$ . SCZOS includes square planar  $(\text{ZnO}_2)^{2-}$  layers and anti-PbO type  $(\text{Cu}_2\text{S}_2)^{2-}$  layers in its layered crystal structure as shown in Figure 1. The  $(\text{ZnO}_2)^{2-}$  layers are similar to  $(\text{CuO}_2)^{2-}$  layers in some superconducting copper oxides, and the  $(\text{Cu}_2\text{S}_2)^{2-}$  layers are the same sublattices seen in  $\text{BaCu}_2\text{S}_2$  and  $\text{LaCuOS}$ .<sup>5,6</sup> These layers may be regarded as functional sublattices intervened by nonfunctional  $\text{Sr}^{2+}$  layers for charge balance.

Transparent p-type conducting properties and room-temperature exciton emission were lately found in the  $\text{LaCuOS}$  oxysulfide with the  $(\text{Cu}_2\text{S}_2)^{2-}$  layers.<sup>7,8</sup> Our recent analysis of the electronic structure of  $\text{LaCuOS}$

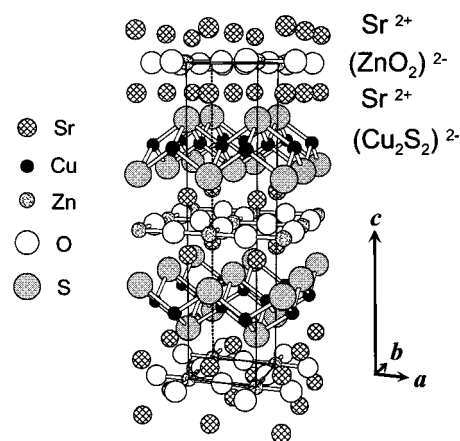


**Figure 1.** Crystal structure of  $\text{Sr}_2\text{Cu}_2\text{ZnO}_2\text{S}_2$  layered oxysulfide.  $\text{Cu}_2\text{S}_2$  and  $\text{ZnO}_2$  layers are separated by Sr layers.

proved that these properties are derived from the  $(\text{Cu}_2\text{S}_2)^{2-}$  layers and its layered structure.<sup>9</sup> Because SCZOS includes the common  $(\text{Cu}_2\text{S}_2)^{2-}$  layers in its crystal structure, the electrical and optical properties similar to  $\text{LaCuOS}$  are anticipated in this material. We previously examined the optoelectronic properties of some Sr–Cu–M–O–S (M = Zn, Ga, In) layered oxysulfides with the  $(\text{Cu}_2\text{S}_2)^{2-}$  layers: SCZOS,  $\text{Sr}_2\text{CuGaO}_3\text{S}$ , and  $\text{Sr}_2\text{CuInO}_3\text{S}$ .<sup>10</sup> This examination revealed that SCZOS is a p-type semiconductor and its electrical conductivity increases by Na-doping. In addition, SCZOS has the largest energy gap among these materials. Although we investigated these electrical and optical properties of nondoped or Na-doped SCZOS, the electronic structure of SCZOS, which will explain the origin of these properties, has not been analyzed yet.

\* To whom correspondence should be addressed. E-mail: kueda1@rlem.titech.ac.jp.

<sup>†</sup> Present address: R&D Center, HOYA Corporation, 3-3-1, Musashino, Akishima, 196-8510, Japan.

(1) (a) Bednorz, J. G.; Müller, K. A. *Z. Phys.* **1986**, *64*, 189. (b) Wu, M. K.; Ashburn, J. R.; Torng, C. J.; Hor, P. H.; Meng, R. L.; Gao, L.; Huang, Z. J.; Wang, Y. Q.; Chu, C. W. *Phys. Rev. Lett.* **1987**, *58*, 908.

(2) (a) Tokura, Y.; Urushibara, A.; Moritomo, Y.; Arima, T.; Asamitsu, A.; Kido, G.; Furukawa, N. *J. Phys. Soc. Jpn.* **1994**, *63*, 3931. (b) Asano, H.; Hayakawa, J.; Matsui, M. *Jpn. J. Appl. Phys.* **1997**, *36*, L104.

(3) Gruner, G. *Density Waves in Solids*; Addison-Wesley Longmans Inc.: Massachusetts, 1994.

(4) Zhu, W. J.; Hor, P. H. *J. Solid State Chem.* **1997**, *130*, 319.

(5) Onoda, M.; Saeki, M. *Mater. Res. Bull.* **1989**, *24*, 1337.

(6) Palazzi, M. C. R. *Acad. Sci.* **1981**, *292*, 789.

(7) Ueda, K.; Inoue, S.; Hirose, S.; Kawazoe, H.; Hosono, H. *Appl. Phys. Lett.* **2000**, *77*, 2701.

(8) Ueda, K.; Inoue, S.; Hosono, H.; Sarukura, N.; Hirano, M. *Appl. Phys. Lett.* **2001**, *78*, 2333.

(9) Inoue, H.; Ueda, K.; Hosono, H.; Hamada, N. *Phys. Rev. B* **2001**, *64*, 245211.

(10) Ueda, K.; Hirose, S.; Kawazoe, H.; Hosono, H. *Chem. Mater.* **2001**, *13*, 1880.

**Table 1. Preparation Conditions of SCZOS Thin Films by RF Sputtering Method**

|                            |  |
|----------------------------|--|
| target                     | SCZOS sintered disk  |
| substrate                  | Al <sub>2</sub> O <sub>3</sub> single crystal: (001) surface |
| substrate temp (°C)        | 580–600  |
| RF power (W)               | 180  |
| atm (vol %)                | Ar/H <sub>2</sub> = 99:1                                     |
| total pressure (Pa)        | 13.3   |
| substrate–target dist (mm) | 30   |

In this paper, normal and inverse photoemission spectroscopy (PES and IPES) measurements were carried out to observe the electronic structure of SCZOS and optical transmission measurements were made to estimate its optical band gap. The observed PES and IPES spectra were interpreted in comparison with the results of the energy band calculations performed by the tight-binding method.

## Experiments

**Preparation of SCZOS Disks and Thin Films.** Sintered disks of SCZOS and Na-doped SCZOS (Sr<sub>1.9</sub>Na<sub>0.1</sub>Cu<sub>2</sub>ZnO<sub>2</sub>S<sub>2</sub>) were prepared by solid-state reaction in the way reported previously.<sup>10</sup> Stoichiometric amounts of SrS, Cu<sub>2</sub>S, Na<sub>2</sub>S, and ZnO powders were thoroughly mixed in a mortar and pressed into disks. The disks were calcined at 920 °C for 4 h in Ar flow. After regrinding them and molding the powder into disks with a cold isostatic press, the disks were sintered at 870 °C for 3 h in Ar flow. Thin films were prepared on sapphire substrates by the radio frequency (RF) sputtering method using the SCZOS sintered disk as a sputtering target. The detailed sputtering conditions are listed in Table 1. The mixed gas of Ar/H<sub>2</sub> = 99:1 was used, and the gas pressure was maintained at 13.3 Pa during film deposition.

**Characterization.** X-ray diffraction (XRD) patterns were measured to examine the purity of the samples. The powder for the XRD measurement was obtained by grinding some sintered disks. The thickness of the film sample was measured by using a stylus. The optical transmission spectrum of the film sample was measured using a conventional UV–vis–near-IR spectrometer.

X-ray photoemission spectroscopy (XPS) and ultraviolet photoemission spectroscopy (UPS) measurements were performed using the excitation lines of Mg K $\alpha$  (1253.6 eV) and He II (40.8 eV), respectively. IPES measurement was carried out in the bremsstrahlung isochromat mode by detecting the photons of 9.5 eV emitted from a sample. The sintered disk of Na-doped SCZOS, which shows the electrical conductivity of  $1.2 \times 10^{-1} \text{ Scm}^{-1}$ , was used as the sample in these measurements to avoid charging. The surface of the sample was scraped with a diamond-impregnated file under the vacuum of  $10^{-8}$  Torr to remove surface contamination before each measurement. The pressure in the analyzing chamber was less than  $5 \times 10^{-8}$  Torr during the measurements. The binding energy ( $E_B$ ) of each spectrum was calibrated by the Fermi energy ( $E_F$ ) of Au.

**Calculation.** The energy band calculation was performed by the tight-binding method. In the tight-binding calculation, O 2s, 2p; S 3s, 3p; Cu 3d, 4s, 4p; Zn 3d, 4s, 4p; and Sr 5s orbitals were used as basis functions. The tight-binding parameters were determined basically in the way proposed by Harrison<sup>11,12</sup> and adjusted to reproduce the evaluated optical band gap and photoemission spectra. The parameters finally adopted are listed in Table 2. The total density of states (DOS) and partial density of states (PDOS) were calculated by summing the number of electronic states in the first Brillouin zone.

(11) Harrison, W. A. *Electronic Structure and the Properties of Solids*; W. H. Freeman and Company: San Francisco, 1980.

(12) Harrison, W. A. *Elementary Electronic Structure*; World Scientific Publishing Co.: Singapore, 1999.

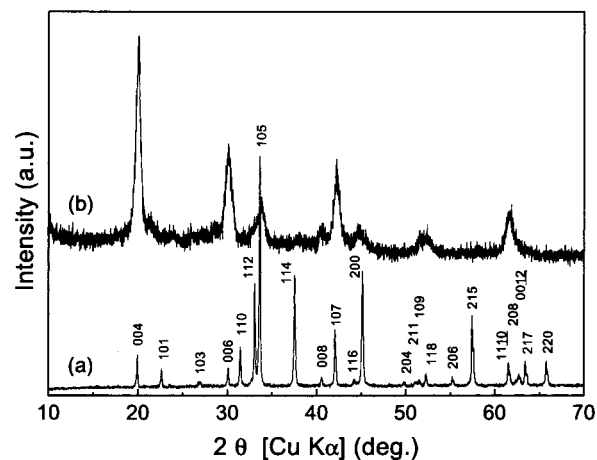


**Figure 2.** XRD patterns of SCZOS: (a) powder and (b) thin film.

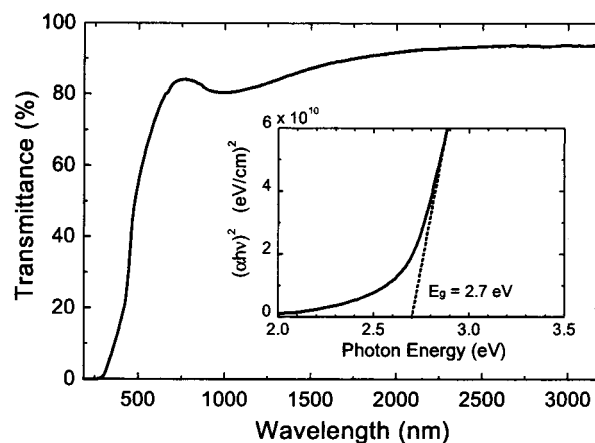


**Figure 3.** Optical transmittance spectrum of SCZOS thin film. The inset shows a  $(\alpha h\nu)^2 - h\nu$  plot to estimate the energy gap.

## Results

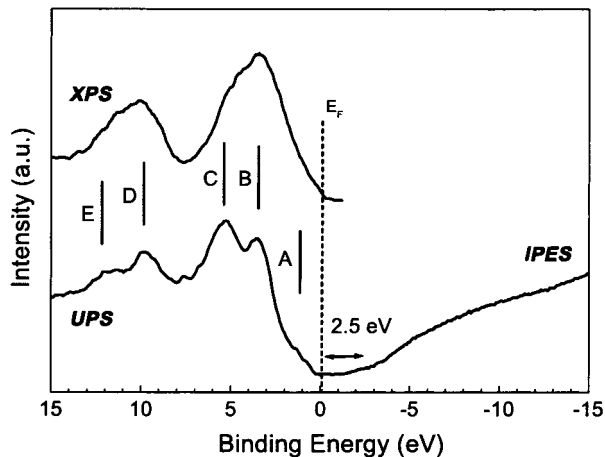
Figure 2 shows XRD patterns of the powder and thin film samples. Every diffraction peak in both patterns was completely indexed according to the patterns calculated by using the cell parameters and atomic coordinates reported by W. J. Zhu et al.<sup>4</sup> No peak arising from other crystalline phases such as SrSO<sub>4</sub> was found in the patterns. In comparison with the powder pattern, the thin film tends to give intense diffraction peaks from (001) planes. The thickness of the thin film measured by a stylus was 180 nm.

Figure 3 shows the optical transmission spectrum of the thin film. The thin film shows high optical transmittance ( $\sim 80\%$ ) in the wavelength region from about 450 to 3200 nm. The absorption edge was found at  $\sim 450$  nm, which agrees with the previous result obtained by the diffuse reflectance of powder samples.<sup>10</sup> The band gap was estimated to be 2.7 eV from the plot of the inset.

XPS, UPS, and IPES spectra are shown in Figure 4. The top of the valence band observed in the XPS and UPS spectra is located at the Fermi level ( $E_B = 0$  eV), while the bottom of the conduction band is seen at approximately 2.5 eV above the Fermi energy ( $E_B \approx -2.5$  eV). These observations explain the wide-gap ( $E_g = 2.7$  eV) and p-type semiconducting nature of SCZOS well in terms of the electronic structure. No sharp structure was resolved in the IPES spectrum. In

**Table 2. Parameters Used in the Tight-binding Band Calculations**

| Parameters for Diagonal Matrix Elements. (eV)    |                     |                     |                     |                     |                     |                     |                    |                    |                    |                    |
|--|---------------------|---------------------|---------------------|---------------------|---------------------|---------------------|--------------------|--------------------|--------------------|--------------------|
| $E_{\text{Sr } 5s}$                              | $E_{\text{Cu } 3d}$ | $E_{\text{Cu } 4s}$ | $E_{\text{Cu } 4p}$ | $E_{\text{Zn } 3d}$ | $E_{\text{Zn } 4s}$ | $E_{\text{Zn } 4p}$ | $E_{\text{S } 3s}$ | $E_{\text{S } 3p}$ | $E_{\text{O } 2s}$ | $E_{\text{O } 2p}$ |
| 4.89   | -3.20               | 3.38                | 8.47                | -9.5                | 1.90                | 6.96                | -7.70              | 0.03               | -18.84             | -5.30              |
| Parameters for Nondiagonal Matrix Elements. (eV) |                     |                     |                     |                     |                     |                     |                    |                    |                    |                    |
|  | $V_{ss\sigma}$      | $V_{sp\sigma}$      | $V_{pp\sigma}$      | $V_{pp\pi}$         | $V_{ds\sigma}$      | $V_{dp\sigma}$      | $V_{dp\pi}$        | $V_{dd\sigma}$     | $V_{dd\pi}$        |                    |
| Zn-O   | -2.523              | 3.316               | 5.841               | -1.46               | -2.772              | 2.329               | 0.522              |                    |                    |                    |
| Cu-S   | -1.671              | 2.197               | 3.867               | -0.967              | -1.358              | 1.268               | 0.211              |                    |                    |                    |
| Sr-O   | -1.608              | 2.114               |                     |                     |                     |                     |                    |                    |                    |                    |
| Cu-Cu  | -1.195              | 1.571               | 2.767               | -0.691              | -0.781              | 0.729               | 0.097              | -0.516             | 0.425              |                    |
| Zn-S   | -0.295              | 0.387               | 0.682               | -0.175              | -0.175              | 0.163               | 0.002              |                    |                    |                    |
| Sr-S   | -1.067              | 1.402               |                     |                     |                     |                     |                    |                    |                    |                    |
| S-S  | -0.100              | 0.132               | 0.232               | -0.058              |                     |                     |                    |                    |                    |                    |
| O-O  | -0.133              | 0.175               | 0.307               | -0.077              |                     |                     |                    |                    |                    |                    |

**Figure 4.** XPS, UPS, and IPES spectra of SCZOS.

contrast to the IPES spectrum, five bands marked as A to E were observed in the XPS and UPS spectra. The three bands, A, B and C, form the valence band, and the other two bands, D and E, form shallow core states.

### Discussion

**Interpretation of PES and IPES Spectra.** We first attempt to interpret the PES and IPES spectra empirically. Taking into account the electronic structures of mono-oxides and mono-sulfides such as Cu<sub>2</sub>O, ZnO, and ZnS,<sup>13-16</sup> it is suggested that the conduction band is formed of Cu 4s<sup>0</sup> and Zn 4s<sup>0</sup> bands, the valence band is composed of Cu 3d<sup>10</sup>, S 3p<sup>6</sup>, and O 2p<sup>6</sup> bands, and the shallow core states consist of Zn 3d<sup>10</sup> and S 3s<sup>2</sup> bands. The shallow core states, D and E, are simply assigned to Zn 3d<sup>10</sup> and S 3s<sup>2</sup> bands from their binding energy and peak intensities. However, the other three bands, A, B and C, in the valence band are not easily assigned in comparison to the electronic structure of the mono-oxides and mono-sulfides, because this material has two anions of O<sup>2-</sup> and S<sup>2-</sup> and the components of the valence band are considered to be highly hybridized. The broad feature in the IPES spectrum does not give any information except that the conduction band consists of fairly dispersed states.

The notable difference between the XPS and UPS spectra in the valence band is the intensity ratio of the band B to the band C; the ratio is remarkably enhanced in the XPS spectrum. The photoionization cross-sections<sup>17</sup> of the Cu 3d, O 2p, and S 3p orbitals, which are denoted by  $\sigma(\text{orbital})$ , are  $\sigma(\text{Cu } 3d) = 9.944 \text{ Mb/atom}$ ,  $\sigma(\text{O } 2p) = 6.816 \text{ Mb/atom}$ , and  $\sigma(\text{S } 3p) = 0.6051 \text{ Mb/atom}$  at the photon energy of 40.8 eV (He II). On the other hand, those are  $\sigma(\text{Cu } 3d) = 0.0148 \text{ Mb/atom}$ ,  $\sigma(\text{O } 2p) = 0.000484 \text{ Mb/atom}$ , and  $\sigma(\text{S } 3p) = 0.001764 \text{ Mb/atom}$  at 1253.6 eV (Mg K $\alpha$ ). Therefore, the band B is tentatively attributed to a Cu 3d band. In addition, it is also implied that O 2p and S 3p orbitals are responsible for the band C and A, respectively, considering the energy levels of these orbitals in atoms: 14.2 eV for O 2p orbitals and 10.3 eV for S 3p orbitals below the vacuum level.<sup>17</sup>

Next, the observed bands are assigned on the basis of the results of the energy band calculation. DOS and PDOS calculated by the tight-binding method are shown in Figure 5, along with the UPS and IPES spectra. The Fermi level observed in the UPS and IPES spectra is set to zero, and the energy of the valence band maximum in the calculated DOS is aligned to zero in the energy scale taking into account the p-type conductive character of SCZOS. The dispersed feature at the bottom of the conduction band in the total DOS is attributed to a broad Zn 4s band by comparison with its PDOS. Cu 4s and 4p bands are located above the Zn 4s band, and the Sr 5s band is found above the Cu 4s band. The upper valence band is composed of well-hybridized Cu 3d and S 3p bands, which give the band A in the PES spectra. The band B in the middle of the valence band mainly consists of a Cu 3d band. The lower valence band, the band C, is assigned to an O 2p band. Two shallow core states, the bands D and E, are attributed to Zn 3d and S 3s bands, respectively. These assignments are consistent with the empirical assignments discussed above.

**Relationship Between Electronic Structure and Electrical Transport Properties.** Transparent n-type conducting oxides such as ZnO usually have a highly dispersed band at the bottom of the conduction band.<sup>18,19</sup> On the other hand, p-type semiconductors with CuS

(13) Robertson, J. *Phys. Rev. B* **1983**, *28*, 3378.(14) Ching, W. Y.; Xu, Y.-N.; Wong, K. W. *Phys. Rev. B* **1989**, *40*, 7684.(15) Ruckh, M.; Schmid, D.; Schock, H. W. *J. Appl. Phys.* **1994**, *76*, 5945.(16) Ley, L.; Pollak, R. A.; McFeely, F. R.; Kowalczyk, S. P.; Shirley, D. A. *Phys. Rev. B* **1974**, *9*, 600.(17) Yeh, J. J. *Atomic Calculation of Photoionization Cross-Sections and Asymmetry Parameters*; Gordon and Breach Science Publishers: Langhorne, PA, 1993.(18) Schröer, P.; Krüger, P.; Pollmann, J. *Phys. Rev. B* **1993**, *47*, 6971.(19) Robertson, J. *J. Phys. C* **1979**, *12*, 4767.



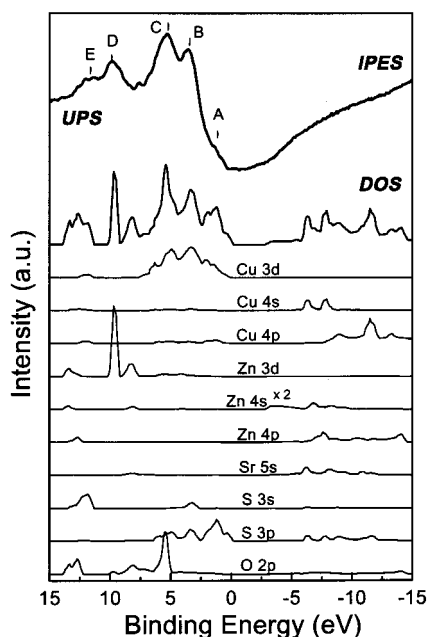


**Figure 5.** Total and partial DOSs calculated by the tight-binding method along with UPS and IPES spectra. The PDOS of the Zn 4s state is doubled in the figure.

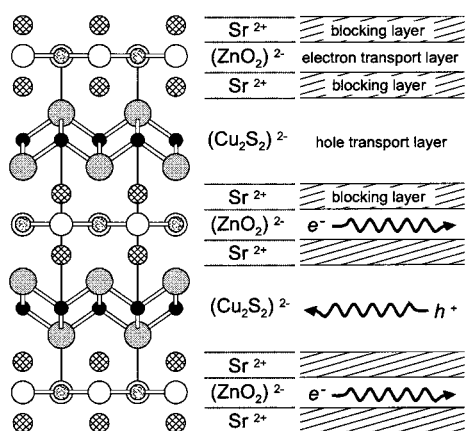


**Figure 6.** Layered crystal structure of SCZOS and electrical transport function anticipated for each layer when electrons or holes are introduced into the respective layer.

layers such as  $\text{BaCu}_2\text{S}_2$  and  $\text{LaCuOS}$  have a hybridized  $(\text{Cu } 3d) - (\text{S } 3p)$  band at the top of the valence band.<sup>9,20</sup> Both of these two features near the band gap are included in SCZOS, because SCZOS has ZnO layers and CuS layers in its layered crystal structure. Therefore, it seems reasonable to consider that SCZOS may show n-type conduction if electrons are introduced into the ZnO layers or p-type conduction if holes are introduced into the CuS layers as shown in Figure 6. However, only p-type electrical conduction was observed in our previous study, even though donor-doping as well as acceptor-doping was attempted.<sup>10</sup>

It is obvious, with respect to hole transport, that the CuS sublattices in SCZOS form the hybridized  $(\text{Cu } 3d) - (\text{S } 3p)$  band in the upper valence band, and the hybridized band is responsible for the p-type electrical conduction in SCZOS. On the other hand, n-type electrical conduction seems to be difficult in this material because

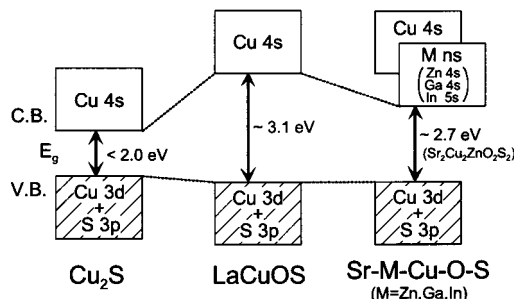


**Figure 7.** Schematic energy band structure of  $\text{Cu}_2\text{S}$ ,  $\text{LaCuOS}$ , and  $\text{Sr-Cu-M-O-S}$  ( $M = \text{Zn, Ga, In}$ ) oxysulfides near the band gap.

donor-doping is usually canceled by the generation of nonintentional and unavoidable Cu vacancies, which compensate carrier electrons.

**Understanding of Electronic Structure in Terms of Layered Crystal Structure.** SCZOS is regarded as a prototype of  $\text{Sr-Cu-M-O-S}$  ( $M = \text{Zn, Ga, In}$ ) layered oxysulfides with CuS layers. Figure 7 illustrates schematic energy band structure of  $\text{Cu}_2\text{S}$ ,  $\text{LaCuOS}$ , and  $\text{Sr-Cu-M-O-S}$  ( $M = \text{Zn, Ga, In}$ ) oxysulfides to interpret the wide-gap properties of  $\text{Sr-Cu-M-O-S}$  ( $M = \text{Zn, Ga, In}$ ) oxysulfides.  $\text{Cu}_2\text{S}$ , which forms into a three-dimensional crystal structure, is well-known as a p-type semiconductor with the small energy gap ( $E_g < 2.0$  eV).<sup>21</sup> The energy band structure of  $\text{Cu}_2\text{S}$  is primarily composed of an unoccupied Cu 4s band and an occupied  $(\text{Cu } 3d) - (\text{S } 3p)$  band.  $\text{LaCuOS}$ , which is a transparent p-type semiconductor, has the largest energy gap ( $E_g = 3.1$  eV) among these materials. This wide-gap character of  $\text{LaCuOS}$  originates from its layered structure composed of CuS layers intervened by highly ionic LaO layers. Since La or O states do not appear near the band gap,<sup>9</sup> the electronic structure of  $\text{LaCuOS}$  near the band gap is simply interpreted by widening the energy gap of  $\text{Cu}_2\text{S}$ .

The energy band structure of SCZOS can be understood in a similar way to  $\text{LaCuOS}$  with respect to their analogous crystal structures, except for a Zn 4s band. The CuS and Sr layers in SCZOS are regarded to correspond to the CuS and LaO layers in  $\text{LaCuOS}$ , respectively. Therefore, these layers give the band structure that is similar to that of  $\text{LaCuOS}$ . However, in the case of SCZOS, the unoccupied Zn 4s band is added beneath the Cu 4s band, forming the bottom of the conduction band. As a result, the energy gap of SCZOS becomes relatively smaller than that of  $\text{LaCuOS}$ . This interpretation is also applied to other  $\text{Sr-Cu-M-O-S}$  ( $M = \text{Ga, In}$ ) layered oxysulfides, in which a Ga 4s or In 5s band replaces the Zn 4s band. Furthermore, the largest band gap of SCZOS among the  $\text{Sr-Cu-M-O-S}$  ( $M = \text{Zn, Ga, In}$ ) layered oxysulfides implies that the Ga 4s or In 5s band is located at a slightly lower energy than the Zn 4s band, and the dispersion of the Ga 4s or In 5s band is larger than that of the Zn 4s band.

## Conclusion

The electronic structure of the SCZOS layered oxysulfide was observed by normal and inverse photoemis-

(20) Ouammou, A.; Mouallem-Bahout, M.; Peña, O.; Halet, J.-F.; Saillard, J.-Y.; Carel, C. *J. Solid State Chem.* **1995**, *117*, 73.

(21) Grozdanov, I. *J. Solid State Chem.* **1995**, *114*, 469.

sion spectroscopy and analyzed by energy band calculations. The energy gap of about 2.5 eV was found in the PES and IPES spectra, and the Fermi energy was located at the top of the valence band. These results agree with the fact that SCZOS is a p-type semiconductor with the optical band gap of 2.7 eV. Five bands, marked as A to E, were observed in the XPS and UPS spectra, and no sharp structure was resolved in the IPES spectrum. Three bands in the valence band, which were located at  $E_B = 1.5$  eV for A, 3.5 eV for B, and 5.2 eV for C, were assigned to the hybridized (Cu 3d)–(S 3p) band, Cu 3d band, and O 2p band, respectively.

The bottom of the conduction band was attributed to the Zn 4s band, and the Cu 4s band was located above the Zn 4s band. The present study of the electronic structure demonstrated that p-type electrical conduction in SCZOS originates from the hybridized (Cu 3d)–(S 3p) band, and the CuS layers can be visualized as the conduction paths for positive holes. Moreover, the wide-gap nature of SCZOS was attributed to its layered crystal structure in comparison with the crystal and electronic structures of Cu<sub>2</sub>S and LaCuOS.

CM0105864